Centrosome amplification favours survival and impairs ovarian cancer progression

Jean-Philippe Morretton[1], Aurélie Herbette[2], Camille Cosson[2], Bassirou Mboup[3], Aurélien Latouche[3], Pierre Gestraud[4], Tatiana Popova[5], Marc-Henri Stern[5], Fariba Nemati[2,6], Didier Decaudin[2,6], Guillaume Bataillon[7], Véronique Becette[7], Didier Meseure[7], André Nicolas[7], Odette Mariani[8], Claire Bonneau[9], Jorge Barbazan[10], Anne Vincent-Salomon[7], Fatima Mechta-Grigoriou[11], Sergio Roman Roman[2], Roman Rouzier[3,9], Xavier Sastre-Garau[7,12], Oumou Goundiam[2,13] and Renata Basto[1,13]

1- Biology of centrosomes and genetic instability, CNRS, UMR144, Institut Curie, PSL Research University, 12 rue Lhomond, 75005 Paris, France.

2- Department of Translational Research, Institut Curie, PSL University, 26 rue d'Ulm, F-75248 Paris Cedex 05, France.

3- Statistical Methods for Precision Medicine, INSERM U900, Institut Curie, 35 Rue Dailly, 92210 Saint-Cloud, France.

4- Bioinformatics and Computational Systems Biology of Cancer, Mines Paristech, INSERM U900, Institut Curie, PSL University, 26 rue d'Ulm, F-75248 Paris Cedex 05, France.

5- DNA Repair & Uveal Melanoma (D.R.U.M.), INSERM U830, Institut Curie, PSL Research University, 26 rue d'Ulm, F-75248 Paris Cedex 05, France.

6- Laboratory of Preclinical Investigation, Department of Translational Research, Institut Curie, PSL University, 26 rue d'Ulm, F-75248 Paris Cedex 05, France.

7- Department of pathology, Institut Curie, 26 rue d'Ulm, F-75248 Paris Cedex 05, France.

8- Biological Resource Center, Department of pathology, Institut Curie, PSL Research University, BRIF BB-0033-00048, 26 rue d'Ulm, 75248 Paris, France.

9- Department of surgery, Institut Curie, 35 Rue Dailly, 92210, Saint-Cloud, France. UFR Simone Veil - Santé, Université Versailles Saint Quentin, Université Paris Saclay, Montigny le Bretonneux, France.

10- Migration and invasion Laboratory, CNRS, UMR144, Institut Curie, PSL Research University, 12 rue Lhomond, 75005 Paris, France.

11- Stress and Cancer Laboratory, INSERM U830, Institut Curie, PSL Research University, 26 rue d'Ulm, Paris, F-75005, France.

12- Present address: Laboratory of pathology, Intercommunal Hospital Center of Creteil, 40 avenue de Verdun, 94010 Creteil Cedex

13- authors for correspondence: oumou.goundiam@curie.fr and renata.basto@curie.fr

Abstract

Centrosome amplification has been described as a common feature of human cancers and it is known to promote tumorigenesis when induced in animals. However, little is known about the real status of centrosome numbers in human cancers and whether numerical alterations are solely associated with poor prognosis. To address this question, we have analyzed a large cohort of human epithelial ovarian cancers (EOCs) from 100 patients using state-of-the-art microscopy to determine the Centrosome-Nucleus Index (CNI) of each tumor. We found that EOCs are highly heterogeneous, with infrequent but strong centrosome amplifications leading to higher CNI than in healthy tissues. Strikingly, while a correlation between CNI and genomic alterations, such as aneuploidy or chromosome rearrangements could not be established, we found that high CNI correlates with increased patient survival and sensitivity to chemotherapy. Using ovarian cancer cellular models to manipulate centrosome numbers and Patient-Derived Xenografts (PDXs), we found that higher CNIs can positively impact the response to chemotherapy and inhibit cell dissemination. Our findings highlight a novel paradigm linking centrosome amplification to the inhibition of tumor progression.

Introduction

The centrosome is the main microtubule (MT) -organizing center of animal cells. Each centrosome is composed of two centrioles surrounded by pericentriolar material (PCM), which is the site of MT nucleation. The centrosome facilitates the accuracy of chromosome segregation during mitosis and influences cell polarity and migration [1-4]. Centrosome duplication is normally tightly controlled to ensure that each centrosome duplicates only once per cell cycle [5,6]. The presence of more than two centrosomes in a cell, centrosome amplification, has long been associated with tumorigenesis, with T. Boveri [7] proposing a link between extra centrosomes, multipolar divisions and consequent aneuploidy. When induced through the manipulation of the centrosome duplication machinery, centrosome amplification, was sufficient to drive tumor formation *in vivo* in a variety of tissues from different animal models [8-12]. Interestingly, although the consequences of centrosome amplification have been normally associated with abnormal cell division and the generation of aneuploidy [7,9,11,12], centrosome amplification can also impact cellular homeostasis in alternative ways. When induced in breast epithelial cells, centrosome amplification resulted in the assembly of invasion-like features, which were RAC1-dependent [13]. More recently, it has been shown that centrosome amplification can drive invasion in a non-cell autonomous manner through increased oxidative stress [14]. Non-cell autonomous detachment of mitotic tumor cells has also been described in organoids containing increased levels of Ninein-like protein, which induces centrosome structural defects [15-17]. Importantly however, even if many studies have described numerical centrosome defects in cultured cancer cells only a limited number of studies tumors has analyzed centrosome number alterations *in situ*.

Epithelial ovarian cancers (EOCs) are the most lethal gynecologic malignancies [18,19]. The high mortality rate is a result of delayed diagnosis and limited therapeutic options despite the use of new drugs, such as the inhibitors of angiogenesis or DNA repair pathways [20,21]. 75% of EOC patients are diagnosed at advanced disease stages, resulting in a 5-year overall survival rate that has recently been improved from 30 to ~47% [22,23]. Histological classification includes mainly serous, endometrioid, mucinous and clear cells carcinomas. The most common EOCs subtype is high-grade serous (HGSOC) which responds at least initially to chemotherapy but presents a worse overall prognosis [24]. Transcriptomic [25-27] and

proteogenomic profiling [28,29] of HGSOC suggested a whole spectrum of molecular diversity that can be linked to patient survival, without yielding a deep understanding of the mechanism leading to relapse [30]. Moreover, up to 50% of HGSOC exhibit defects in homologous recombination (HR) pathways [26]. HR deficient (HRD) patients with germline or somatic mutations in *BRCA1/2* genes are known to be more sensitive to platinum-based chemotherapy and Parp inhibitors than non-BRCA-mutated tumors [19,21,31] more broadly defined as the HR proficient (HRP) patients. Since EOCs are characterized by high level of genomic alterations [26,32] and centrosome numerical defects are associated with aneuploidy, we characterized a large cohort of 100 naive EOCs, comprising 88 HGSOCs, using immunofluorescence and state-of-the-art microscopy. For each tumor, we established the centrosome-nucleus index (CNI) as a proxy to compare centrosome numbers among our cohort. Surprisingly, we found that the frequency of centrosome amplification was less important than what is predicted from the literature. Integration of CNI data with genomic and clinical data revealed a striking association between centrosome amplification and patient outcome. Using patient-derived xenografts (PDXs) and cell line models, we showed that centrosome amplification can positively influence the response to chemotherapy, while it can also inhibit tumor cell dissemination through the mesothelium. Our results demonstrated for the first time that centrosome amplification is not associated with a worse prognosis, but more surprising, they show that decreased centrosome numbers, translate in poorer response to chemotherapy and increased capacity of tumor cell invasion. Overall this study identifies decreased centrosome numbers, but not centrosome amplification, as a condition that favours ovarian cancer progression.

Results

Characterization of centrosome defects in human epithelial ovarian cancer (EOC) tissues

In order to analyze centrosomes in human epithelial ovarian cancers (EOCs), we designed a strategy where 20μm frozen tissue sections were obtained by the pathology department of Institut Curie. These were previously categorized as healthy tissues (corresponding to healthy ovaries from prophylactic oophorectomy or hysterectomy removal) or tumor tissues, which enclosed a mix of serous (90%), endometrioid (3%), mucinous (4%) and clear cell carcinoma (3%) (methods and Supplementary Table 1). Importantly, all tumors were naïve, obtained after surgery without previous neo-adjuvant chemotherapy. Tissues were methanol fixed and processed for immunostaining with two different antibodies CDK5RAP2 and pericentrin (PCNT), two PCM components, to unambiguously identify centrosomes through co-localization. Confocal microscopy was used to obtain optical sections from ten random fields in the entire tissue (Figure 1A). Analysis of healthy tissues allowed us to identify centrosomes through the co-localization of the two centrosomes markers (Figure 1B). We also noticed the presence of structures that only contained one of the two centrosome markers (Figure 1B), and importantly, these were not considered as centrosomes. To further characterize and confirm the centrosomal configurations described above, we used 3D structural illumination microscopy (3D-SIM) of ovarian tissues immunostained with the centriolar marker-Cep135 and PCNT, allowing higher resolution for both centrioles and PCM (Figure 1D). To our knowledge this represents the first centrosome super resolution analysis performed in human tissues and tumors. We found that in healthy tissues, each centrosome contained two centrioles and that PCNT surrounded one of the two centrioles, presumably the mother centriole (Figure 1D), as expected [33].

Analysis of tumor tissues revealed the presence of highly heterogeneous conditions with several centrosome abnormalities. Extra centrosomes were easily identified by the presence of multiple CDK5RAP2-PCNT positive co-localizing structures associated with one nucleus (Figure 1C). In certain cells, ECs were isolated and spread away from each other (Figure 1C- top panel) and these were named isolated centrosomes. In other cells, extra centrosomes were clustered together- clustered centrosomes (Figure 1C, middle panel). Interestingly, we also

observed a configuration that to our knowledge has never been described before, where ECs were tightly associated in a single structure appearing very tightly clustered and hence named super-clusters (Figure 1C lower panel). SIM analysis of these tumors, with the markers described above confirmed the aberrant extra centrosome morphologies (Figure 1E).

We next quantified the frequency of these defects in a cohort of 19 healthy tissues and 100 tumor tissues. We imaged ten random different fields, corresponding to different regions of the tumor. Importantly, we only imaged and analyzed regions corresponding exclusively to the tumor tissue, excluding regions of stromal tissue that normally surround the tumor. Interestingly, while the majority of tumors (60%) presented at least one of the defects described above in terms of centrosome number, whereas the remaining 40% of tumors did not show any of these defects (Figure 1F). This type of centrosome numerical aberration was never observed in healthy tissues. Still considering only the different type of ECs configurations found in tumors, we observed that 18% of the tumors (n=18, from 100) presented the three categories: isolated, clustered and super-clustered (Figure 1G).

All together, the methodology employed to analyse 100 ovarian tumors and comparison with ovarian healthy tissues revealed the presence of centrosome number abnormalities in a large fraction of EOCs.

Extra centrosomes are present in the large majority of EOCs, but high levels of centrosome amplification are infrequent

We next focused our analysis in the quantification of centrosome number abnormalities in tumors. Tumor tissues appeared very disorganized and it was difficult to ascertain the number of centrosomes per cell as in many cases, centrosomes were not closely associated with the nucleus. To unambiguously quantify centrosome number and to be able to compare all tumors and healthy tissues, we visually counted the number of nuclei and the number of centrosomes in each of the ten randomly chosen fields, and determined the Centrosome Nuclei Index (CNI) by dividing the number of centrosomes by the number of nuclei. It is important to mention that we tried to automatize centrosome and nuclear segmentation followed by quantification. This approach was however far from reproducing the manual counting, with a strong bias towards considering unrelated

structures as centrosomes. The data we present therefore results from manual counting.

Overall our analysis comprised a total of 653627 nuclei, 874766 centrosomes from 1174 fields, with an average of 5248 nuclei counted per tumor. In healthy tissues, the average CNI was 1.02±0.02 and it was relatively stable, varying from 0.81 to 1.16 (Figure 2A). In tumors, however, the CNI was much more variable. On average, 1.43±0.038, with the minimum 0.61 and maximum at 2.55. Interestingly, 89% (n=89 out of 100) of the tumors presented a CNI superior to the average CNI found in healthy tissues (Figure 2A, yellow dashed line and Supplementary Figure 1A). However, only 9% (n=9 out of 100) of tumor tissues exhibited centrosome amplification (Figure 2A, green dashed line), when defined by the presence of more than two centrosomes in a cell [7,34,35]. We also investigated the frequency of extra centrosomes clusters and super-clusters per nuclei, and found that they were extremely uncommon (0.71%±0.09 for clusters and 0.72%±0.08 for super-clusters) (Supplementary Figure 1B), confirming the low frequencies of extra centrosomes in these tumors.

We next dichotomized our population in two groups using Classification And Regression Trees (CART) methods [36], restricting the analysis to the high-grade serous ovarian cancers (HGSOCs) within our cohort. These represented the majority of the tumors- 88%, which is also the case worldwide for EOCs [24]. This resulted in the categorization of the cohort into low CNI (≤ 1.45) and high CNI (> 1.45), with 55 tumors falling into the low CNI category, while 33 were placed in the high CNI category (Figure 2A, red line).

We first investigated whether the dichotomization of our tumor cohort in low and high CNI identified any preference for the different extra centrosome categories (isolated, cluster and super-cluster) identified by microscopy. Using multivariated analysis, we recognized a significant trend for isolated centrosomes and clusters (p= 0.021 and p= 0.035 respectively, Supplementary Figure 1C) to be associated with high CNI tumors. Interestingly however, even if not statistically significant, super-clusters were associated with low CNI tumors (p=0.0788, ns). To gain more information about the distribution of structures containing extra centrosomes, we plotted the number of clusters and super-clusters (as the structures that contain more centrosomes) in parallel to the CNI analysis (Figure 2B). We found that certain

tumors with low CNI (placed at the bottom of the graph) contained clusters and super-clusters at similar frequencies as tumor tissues placed at the other end of the graph. We hypothesized that low CNI tumors containing the same frequencies of extra centrosomes than high CNI tumors, should contain cells without centrosomes. Corroborating this hypothesis, we could easily identify regions without centrosomes (Supplementary Figure 1D) in tumors with low CNI values.

We concluded that EOCs are highly heterogeneous in terms of centrosome numbers, and surprisingly only a small population of tumor cells display extra centrosomes.

The CNI does not correlate with proliferation, mitotic indexes, genomic alterations or transcriptomic changes in HGSOCs

We next wanted to study the possible correlation between CNI and different molecular and clinical parameters. We analyzed whether the CNI status correlated with proliferation. We used two indicators, the mitotic index (MI) and, the proliferation marker Ki67 by H&E staining and immunochemistry respectively. Interestingly, we did not find any correlation between CNI and MI or Ki67 (Supplementary Figure 2A-B), suggesting that both CNI low and CNI high tumors show similar proliferative and mitotic indexes.

Genomic alterations are frequently found in HGSOCs [26,32]. Centrosome defects can lead to mitotic errors, chromosome instability and aneuploidy [37,38]. In order to identify a possible link between centrosome number and genomic alterations, we used high resolution Cytoscan arrays and GAP tools [39]. With these tools, we analyzed information related with chromosome content (ploidy) and the presence of small and/or large DNA structural rearrangements. Importantly, we did not find any correlation between CNI status and ploidy, chromosome number and DNA structural rearrangements (Supplementary Figure 2C-F). We concluded that small or large chromosome breaks were not associated with low and high CNI tumors.

Different pan-cancer studies [40,41] have shown that whole genome duplications (WGD) precedes many different types of genomic alterations. WGDs might represent a mechanism to generate aneuploidy, leading to chromosome number reduction, as shown in a mouse ovarian cancer model [42]. WGD-positive (near tetraploid) tumors contain a ploidy of 3.31 on average, while ploidy is closer to ~1.99 (near diploid) for

WGD-negative tumors [41]. Centrosome amplification and WGD are hallmarks that have been associated, as both can be produced via the same mechanisms such as cytokinesis failure [40]. We therefore examined if CNI correlated with ploidy in our tumor cohort. We found that this was not the case (Supplementary Figure 2G), even if we noticed that tumors with low CNI contained twice more near tetraploid (67%, n=26 out of 39 total tumors), than near diploid karyotypes (33%, n=13 out of 39 total tumors). In tumors with high CNI however, the distribution was similar for near tetraploid (46%, n=13 out 28 total tumors) and for near diploid (54%, n=15 out of 28 total tumors), (Supplementary Figure 2G). This suggests that cytokinesis failure is not the only mechanistic explanation for extra centrosome accumulation, or that there are yet unidentified centrosome reduction mechanisms at play. Moreover, even if not statistically significant, low CNI seems to be associated with WGD and hence with worse clinical prognosis [40].

We also analyzed the transcriptome of our cohort using Affymetrix U133Plus2.0 microarray technology with the aim of identifying altered transcriptomic signatures. Interestingly, we did not find any major differences in gene expression between low and high CNI tumors, even when considering the extreme low or high CNI HGSOCs (not shown). We next compared with published HGSOCs transcriptome signatures, which have described fibrosis and stress profiles due to the expression of mesenchymal and oxidative stress genes, respectively [25]. We found that while high CNI tumors display equivalent distributions between fibrosis and stress tumors, a tendency for fibrosis (63%, n=29 out of 46) was found in low CNI tumors (Supplementary Figure 2H). We conclude that no major transcriptomic alterations correlate with CNI. Interestingly however, low CNI tumors seem to display characteristics typical of fibrosis type, which are of poor prognosis.

High CNI correlates with better overall survival and response to chemotherapy in HGSOCs

The results described above suggested that low CNI is associated with worse prognosis. To independently test this possibility, we plotted patient survival curves according to the CNI status. We found that low CNI was associated with worse overall survival (Figure 3A, Log-rank test: p=0.018, HR=1.931, 95% CI=[1.14-3.28]) and furthermore with an increased risk of relapse, (Figure 3B, Log-rank test: p=0.018, HR=1.706, 95% CI=[1.06-2.75]). In contrast, high CNI was associated with

better overall survival. To avoid any bias due to tumour stage in the prognostic value of CNI, we thus investigated whether the CNI status reflected FIGO staging [43]). Importantly, we found that both low and high CNI tumors could be identified at all stages (I to IV) (Supplementary Figure 3A). Interestingly, the majority of the cases in our cohort correspond to stage III (59.0%, Supplementary Table 1) and these comprise once more low and high CNI tumours. We concluded that the association between high CNI and patient survival does not depend on tumor stage.

Relapse is a challenging situation in HGSOCs. Patients are categorized according to their response to chemotherapy and women who relapse within 6 months after the completion of the first line of chemotherapy are defined as platinum resistants [44]. We tested if the CNI parameter can be used as an indicator of relapse, defining early and late as before or after 6 months. We used predictiveness curves [45] to evaluate the performance (robustness) of the CNI as a classifier and the optimum threshold allowing to stratify patients according to relapse. We performed this analysis taking into consideration the presence of extra centrosomes, since 63% (n=56 out of 88) of our HGSOC cohort harbour these defects. Using boostrap resampling process, our predictiveness curves showed that the optimum CNI value is 1.456 (95% CI=[1.22-1.76], Supplementary figure 3B). This optimum value confirmed the threshold of 1.45 established previously to define low and high CNI tumors. Taken together our study shows for the first time that centrosome numbers can be used as an indicator of disease recurrence in HGSOC. Furthermore, these results clearly demonstrate the prognostic value of CNI status in HGSOC for patient survival and response to treatment. Unexpectedly, they also show that low CNI, and so reduced centrosome numbers are associated with worse prognosis.

High CNI tumors include more cases with homologous recombination deficiency

Mutations in genes encoding members of the DNA damage repair (DDR) pathway such as BRCA1 and BRCA2 (BRCA1/2), which are involved in homologous recombination (HR) lead to increased risk of breast and ovarian cancers [46]. Interestingly however, patients harbouring HR deficiency (HRD) are more sensitive to platinum, one of the two main chemotherapy for EOCs. We investigated whether there was an association between HRD and CNI status using the Large-scale transition (LST) genomic signature [47,48]. This signature is based on the presence of

large-scale chromosome breakpoints of at least 10Mb, which is an indicator of HRD. While low CNI status contained similar distributions of HRD and HR proficient (HRP) tumors (45% and 55% respectively), high CNI was mainly associated with HRD tumors (74% HRD and 26% HRP, respectively p= 0.024) (Figure 3C). Importantly, analysis of HRD patient overall survival did not show any significant association with the CNI status (Figure 3D, p=0.648, HR=1.229 and 95% CI=[0.49-3.17]). However, HRP patients showed significant differences according to CNI (Figure 3E p=0.0372, HR=2.644 and 95% CI=[1.11-6.2]), suggesting that this index can be used to stratify HRP patients. Overall, these results show that an increase in the number of centrosomes within a tumor can be beneficial for the patient. Further, while the CNI status does not seem to be a parameter to take into consideration in HRD patient survival (the ones that respond better to treatment), it can differentiate less sensitive HRP patients.

Investigating the effect of chemotherapy according to CNI

The treatment of EOCs relies on a combination of platinum and taxane derivative agents, which target DNA integrity and the microtubule cytoskeleton respectively [44]. We wondered whether there was an association between the CNI and the response to chemotherapy, which could explain the different response to treatment in patients with low and high CNI. We first tested the effect of a combination of carboplatin and paclitaxel in cells lines, where centrosome number can be easily manipulated. In order to increase centrosome number, we generated iOVCAR8-Plk4 and iSKOV3-Plk4 stable cells lines, where the over-expression of Plk4 (Plk4OE), the master centriole duplication kinase can be induced with Doxycycline (Dox) (hence referred to as Plk4OE+), a strategy previously used to amplify centrosomes (Figure 4A) [49]. Centrinone, a Plk4 inhibitor [50] was used to decrease centrosome numbers (Figure 4A), and it will be referred to as centrinone cells. Treatment of either cell line with Dox and centrinone effectively impacted the CNI (Figure 4B and Supplementary Figure 4A-B). Although proliferation was decreased in Plk4OE+ and centrinone treated cells, these still proliferated (Supplementary Figure 4C-D) and the levels of apoptosis were only mildly increased (Supplementary Figure 4E). OVCAR8 and SKOV3 are HGSOC cell lines containing mutations in p53 [51], explaining the lack of response to centrosome number alterations, in contrast to diploid untransformed cell lines [50,52,53].

We next determined the IC50 relative to carboplatin or paclitaxel for each cell line according to CNI status. In order to define efficient concentrations required to induce optimum cell growth inhibition, different concentrations of each drug including IC50 were used for drug combination optimization. Treatment of iOVCAR8-Plk4OE+ cells significantly impacted cell viability, while there was no additional effect on iOVCAR8 with reduced centrosome numbers, which was similar to controls (Ctrls) or to cells treated with DMSO (Figure 4C-D). Interestingly, treatment of iSKOV3 cells did not impact their viability (Figure 4E-F). We concluded that only iOVCAR8-Plk4OE+ (manipulated to contain a higher CNI- centrosome amplification) showed increased sensitivity to combined chemotherapy.

We next investigated the effect of chemotherapy *in vivo*, using two Patient-Derived Xenografts (PDXs) derived from two tumors from our cohort with distinct CNIs (Figure 4G-I). Importantly, to avoid any bias due to platinum sensitivity known for HRD tumors, we selected in our study two PDXs models derived from HRP tumors. Chemotherapies were administered intraperitoneally either every three weeks (carboplatin) or weekly (paclitaxel) during 6 weeks. Tumor growth was assessed until the tumor reached a volume of 2500 mm^3, as stipulated by ethical regulations. The effect of chemotherapy on tumor growth was determined by the median period of time required to reach a 4 fold increase in tumor volume (RTVx4). Analysis of the median time showed that chemotherapy inhibited tumor proliferation of both ovarian PDXs. However, while the delay to reach RTVx4 comprised 20 days in the low CNI PDX OV014 compared to control (Figure 4J, Log-rank test: p=0.0013, HR=3.552, 95% CI=[2.47-20.3]), it was extended to 51 days in the high CNI PDX OV026 compared to the control (Figure 4K, Log-rank test: p=0.0005, HR=4.306, 95% CI=[3.925-58.50]). These results suggest that combined chemotherapy delays more significantly the growth of PDXs with higher CNI.

Low CNI ovarian cancer cells cause more efficient mesothelial cell clearance

It has been shown that centrosome amplification induces invasive oncogenic-like features in a 3-D culture mammary cell (MCF10A) model, both in cell or non-cell autonomous manner [13,14]. Importantly, the levels of an activated form of RAC1, a small GTPase with described oncogenic signalling properties [13], were increased. We thus tested whether centrosome number alterations lead to RAC1 activation in ovarian cancer cell lines. We did not observe any significant difference in activated

RAC1 levels in response to Dox or centrinone treatment (Supplementary Figure 5A-D). Thus, the differences observed between these two experimental condition seem to be justified by differential tissue specific responses to centrosome numerical alterations, as already described in flies and mice [8,9,11,12,35,54].

EOCs undergo a particular mode of motility, where tumor cell invade the peritoneal cavity through a process called tumor dissemination [55]. Indeed tumor cells detach from the primary tumor site, adhere and go through mesothelial cells that enclose peritoneal organs [56]. Since centrosome number alterations have been shown to impact cell migration and invasion [3,13,57], we hypothesized that differences in centrosome number might influence the capacity of ovarian cancer cells to invade the mesothelial barrier. We performed *in vitro* mesothelial clearance assays using ovarian cancer spheroids derived from iOVCAR8-Plk4 and iSKOV3-Plk4 described above (Figure 5A). Cells were treated for 4 days with Dox or centrinone to induce centrosome number alterations. In the last two days, they were plated on polyHEMA, to induce spheroid assembly. Importantly, we verified that this treatment did not influence centrosome number in any of the tested conditions (Supplementary Figure 6C-E). To perform the clearance assays we differentially labelled tumor spheroids, and mesothelial cells previously plated on collagen-coated surfaces. The capacity to clear and invade this layer of cells was measured over time (Figure 5B-C), as described in [58]. Both iOVCAR8 or iSKOV3 cells with or without DMSO showed comparable mesothelial clearance capacity. Interestingly, iOVCAR8-Plk4OE+ or iSKOV3-Plk4OE+, with extra centrosomes showed decreased capacity to clear. Strikingly, centrinone treatment increased the clearance capacity in both cell lines, with a more pronounced effect of iSKOV3 spheroids (Figure 5D, Supplementary Figure 6A-B and Supplementary videos 1-8). Statistical analysis (methods) revealed a significant difference in clearance capacity between Ctrl and Plk4OE+ cells. Importantly, and surprisingly, centrinone treated cells, showed increased clearance capacity when compared with DMSO treated cells.

Our results showed that tumor spheroids with reduced centrosome number displayed increased clearance capacity, while the presence of extra centrosomes induced the opposite behaviour. We wanted to compare heterogeneous spheroids that contained a mixed cell population in terms of centrosome number. We generated two types of spheroids for iOVCAR8 and iSKOV3 cells containing either a mix of Ctrl cells with Plk4OE+ or Ctrl cells with centrinone treated cells. In each

spheroid, cells were differentially labelled with green and red cell dyes before platting them on mesothelial cells labelled in blue. We confirmed that each treatment resulted in the expected alteration of centrosome number of the mixed spheroids (Supplementary Figure 6H-I). We then analyzed clearance capacity as described above. Interestingly, mixed spheroids containing centrinone treated cells cleared less efficiently than spheroids containing exclusively centrinone-treated cells. Remarkably however, these mixed spheroids remained more capable of clearing mesothelial cells than any spheroids that did not contain cells without centrosomes, highlighting the capacity for ovarian cancer cells with reduced centrosome numbers to drive clearance (Figure 5E, Supplementary Figures 6F-G and Supplementary videos 9-12).

Together, the mesothelial clearance assays described above shows that ovarian cancer cells with extra centrosomes seem to display a disadvantage in terms of cancer cell dissemination through mesothelial cells. Strikingly, our results also show that low CNI spheroids have a significant advantage (presented by two distinct cell lines), suggesting that low CNI cells might be the ones that considerably contribute to the metastatic process in HGSOCs.

Discussion

Whereas centrosome number alterations, namely centrosome amplification, has been shown to be sufficient to initiate tumorigenesis in animals [8-12], the frequency of centrosome amplification in human tumors has remained under investigated. Here, we analyzed a large cohort of human ovarian tumors and we found that centrosome amplification is less frequent than what has been found in most human cancer cell lines, including ovarian cancer cell lines ([59] and this study- where CNI determination has been used for HGSOCs). Importantly, our study shows a higher heterogeneity in the number of centrosomes in ovarian tumors, with certain nuclei presenting over 15 centrosomes, while others even lack centrosomes. Tumor heterogeneity has been reported for many different tumor features and this work shows that heterogeneity of centrosome numbers is a hallmark of ovarian tumors.

Centrosome amplification has been correlated with aneuploidy and chromosome instability, however, a correlation between centrosome number increase and aneuploidy was not found in this cohort. These results suggest that even if centrosome amplification might contribute to chromosome number alterations, this is not the only mean by which ovarian tumors become aneuploid. Furthermore, our work also suggests that centrosome numbers do not influence the global rate of proliferation as revealed by Ki67 and mitotic index analyses. In vertebrates, p53 inhibits the proliferation of cells lacking centrosomes [50] and in cells with extra centrosomes [49,60]. However since p53, is found mutated in the large majority of ovarian tumors [26], centrosome number alterations most likely do not influence cell cycle progression or trigger cell cycle arrest.

Although still limited to a few tumor types, observations in certain tumors or in cancer cell lines derived from advanced tumors grades have suggested that centrosome amplification is correlated with advanced tumor stages and worse tumor prognosis [61]. Surprisingly, however, in the EOC cohort analyzed in this study, which comprises in its large majority high-grade tumors, centrosome amplification was not frequent. And more surprisingly, increased centrosome numbers in high CNI tumors correlated with better prognosis. Patient overall survival was increased in tumors with high CNI, and time to relapse, was also found to be increased in the same group of patients. In contrast, patients with low CNI presented decreased survival and showed short-term relapse (Figure 6).

It is possible that many different factors contribute to the positive association between high CNI and patient outcome in EOCs identified in this study. Our work has identified two important contributions. The first one is related with chemotherapy. We found that both in PDXs and in one ovarian cell line (OVCAR8), centrosome amplification delays tumor growth and decreases cell viability. This chemosensitivity is not due to HRD status since we used two PDXs models derived from HRP tumors, the ones that present worse prognosis. The fact that centrosome amplification did not influence chemotherapy in SKOV3 cell lines, suggests the contribution of differences in the genetic background of each cell line. Additional experiments should address the mechanisms underlying chemotherapy sensitivity in ovarian cancer cells with extra centrosomes. Since taxol targets and stabilizes the microtubule cytoskeleton, it is tempting to speculate that the combination of extra centrosomes and taxol might inhibit centrosome clustering, leading to multipolar cell division and so decreasing tumor cell viability [62].

The findings that ovarian cancer cell lines containing extra centrosomes showed decreased mesothelial cell clearance capacity was surprising in light of the results found in breast cells [13,14], suggesting once more that tissue specific properties influence the consequences of altered centrosome numbers. Ovarian tumors do not show typical invasion features seen in other tumor types [63]. Indeed peritoneal metastases via transcoelomic dissemination appear to be a characteristic of HGSOCs [55,64], where tumor cells detach from the primary tumor, using the ascitic fluid as a carrier to reach mesothelial cells that line the peritoneal cavity [56,65]. Importantly however, we show that decreased centrosome number confers an advantage to ovarian cancer cell dissemination (Figure 6). These results, together with the results described above, support the importance of characterizing centrosome numbers and its association with survival and relapse in light of cancer treatment possibilities. It has been suggested that inhibition of centrosome clustering or centrosome duplication might represent treatment opportunities to inhibit the proliferation of cancer cells with extra centrosomes [34,35,66]. Our results suggest that, at least in ovarian cancer, this type of therapy might inhibit the response to chemotherapy or even fuel the capacity of cancer cells to invade, with catastrophic outcome to the patient.

The results showing increased chemosensitivity of cancer cells and the PDX with high CNI should be consider within the context of possible chemotherapy side

effects. If in heterogeneous primary tumors, cells with increased centrosome numbers are more susceptible of being eliminated after chemotherapy, this might result in the selection of cells with normal or low centrosome numbers. These cells show increased invasion capacity and so might represent an additional burden as they will favor metastatic behavior and relapse.

Another important finding of this work is the possibility of using centrosome number and in particular the CNI, as a prognostic tool. This might be quite advantageous to clinically manage patients according to CNI status, in particular in light of emerging novel therapies such as Parp inhibitors or others [67]. It is possible that the use of CNI, in addition to genomic signatures might be beneficial in HGSOCs, which lack bona fide biomarkers and limited therapeutic options [68].

Figure legends

Figure 1. Characterization of centrosome numbers in EOCs

(A) Schematic diagram of the workflow used to analyze ovarian tissue sections. Frozen healthy or tumor ovarian tissues were sectioned into 20μm thickness sections and methanol fixed. These were subsequently immunostained for two centrosomes markers and nuclei were labeled with DAPI. Ten random fields were imaged through the entire Z-stack using confocal microscopy. Each field was analyzed and centrosomes and nuclei were quantified visually. (B-C) On the left, representative micrographs of low magnification views of healthy (B) and tumor tissues (C) immunostained with antibodies against pericentrin (PCNT) and CDK5RAP2, show in red and green respectively. DNA in blue. The white dashed squares represent the regions shown in higher magnification on the right. One centrosome was considered as such when PCNT and CDK5RAP2 signals co-localized. Lack of co-localization was noticed (B) and discarded for quantification. In tumors (C), extra centrosomes could be noticed and were present in three different configurations: isolated centrosomes (top), when more than two centrosomes were present and easily distinguished as well separated entities; clusters when extra centrosomes were present and remained closely associated and super-clusters when extra centrosomes were tightly packed and found close to each other. (D-E) Super resolution microscopy of healthy tissues (D) and tumor tissues (E) immunostained for the centriole marker Cep135 and PCNT. In normal tissues, two centrioles showing asymmetric PCM localization are detected, while in tumors (E), the three different configurations described above for extra centrosomes can be seen, with two centrioles forming each centrosome in the isolated centrosome category, many clustered centrioles in the cluster category and even more in the super-clustered configuration. (F) Graph bar showing the percentage of tissues with and without extra centrosomes. (G) Venn diagram illustrating the overlap of the different extra centrosome categories in tumors.

Figure 2. Characterization of the Centrosome Nuclei Index (CNI) in healthy and tumor tissues

(A) Plot showing the CNI value of all 100 tumors (blue) positioned in ascending value and 19 healthy tissues (yellow) analysed. The yellow dash line represents the average CNI value of all normal tissues analysed (1.02) and the red line the threshold of CNI value defining HGSOCs as low or high CNI tumors (1.43). The green dash line represents centrosome amplification as defined by the literature (>2 centrosomes in the cell). (B) Plot showing the total number of clusters and super-clusters identified in tumors. Note that the order of the tumors is conserved between the two plots to allow for comparison between the CNI and the number of extra centrosomes within the same tumor.

Figure 3. Higher CNI correlates with increased survival and time to relapse

(A-B) Kaplan-Meier curves showing patient overall survival (A) and the percentage of patients without relapse, after the first line of chemotherapy (B) according to CNI status. Statistical significance was assessed with Log-rank test for group comparison. (C) Contingency table showing the distribution of HR proficient (HRP) or deficient (HRD) in low and high CNI tumors. p value from Fisher's exact test. (D-E) Kaplan-Meier curves showing patient overall survival according to CNI status in HRD (D) and HRP (E) patients. Statistical significance was assessed with Log-rank test.

Figure 4. Chemotherapy inhibits growth of ovarian cancer cell lines and PDXs with extra centrosomes

(A) Schematic diagram of the generation of iOVCAR8 and iSKOV3 cells lines. OVCAR8 and SKOV3 cells lines were infected with lentiviral vector expressing the full length Plk4 construct. After selection, positive clones of inducible iOVCAR8 and iSKOV3 were isolated. These cells are referred to as control (Ctrl) cells. Addition of doxycycline (Dox+) generates Plk4OE+ cells. Treatment of Ctrl cells with centrinone reduces centrosome numbers and DMSO was used as control. (B) Graph bars plotting the CNIs of iOVCAR8 (left) and iSKOV3 (right) after Dox+, DMSO or Centrinone treatments. p value from one-way ANOVA (C-F). Graph bars plotting the percentage of viable cells in iOVCAR8 (C-D) and iSKOV3 (E-F) after the indicated chemotherapy treatment for 72 hours. Note that non-treated cells were used as

reference (100% viability), n=3 independent experiments. Statistical significance was assessed by a Wilcoxon test. (G) Schematic diagram of ovarian tumor engraftment in mouse and chemotherapy in PDXs. (H) Graph bar showing the CNIs of the tumors and corresponding PDXs. 10 fields from each PDX were quantified in a total of 9204 nuclei. Statistical significance was assessed with Mann-Whitney test. (I) Representative micrographs of tumors and the corresponding PDXs labeled with PCNT (red) and CDK5RAP2 (green) antibodies. (J-K) Kaplan-Meier curves illustrating the time elapsed to reach 4X the initial tumor volume in Ctrl or chemotherapy treated PDXs with low (J) or high (K) CNIs. The black line indicates the median time (in days) to reach RTVx4 under chemotherapy compared *to* Ctrl: 20 days for Low CNI PDXs and 51 days for High CNI PDXs. p value from Log-rank test.

Figure 5. Ovarian cancer cell lines with low CNI show improved capacity to clear through mesothelial cells

(A) Schematic diagram of workflow. Ovarian cancer cell lines were grown on polyHEMA to form spheroids and were labeled in red. Mesothelial cells were labeled in green and plated as monolayers on collagen I coated surfaces. The CNI was validated for each experiment by immunofluorescence microscopy. Ovarian spheroids were plated on mesothelial cells and imaged for 16hrs in time-lapse movies. The normalized clearance quantification was determined by dividing the hole size at different time points by the initial spheroid size. (B) Stills of a time-lapse movie of Ctrl spheroids (labeled in red in the merged figures and shown in grey on the top panel) and mesothelial cells (labeled in green in the merge figures and shown in grey on the middle panel). Time is shown in hours (h). (C) z- view of Ctrl cells as shown in B. Note the red cells at the beginning of the movie on top of the mesothelial layer while at later time points they have cleared through the mesothelial cells. (D) Graph bars of the normalized clearance in A.U. of iOVCAR8 (left) and iSKOV3 (right) spheroids after the indicated treatments. For each experimental condition 45 different spheroids were analyzed from three independent experiment. Statistical significance was assessed with ANCOVA test. (E) Graph bars of the normalized clearance in A.U. of iOVCAR8 (left) and iSKOV3 (right) spheroids after the indicated treatments or in mixed spheroids of the indicated treatments. For each experimental condition 30 different spheroids were analyzed from three independent experiments. Statistical significance was assessed with ANCOVA test.

Figure 6. Model of the impact of centrosome alterations in HGSOCs

In our cohort of HGSOCs we have identified two sub-populations of tumors. One with high and one with low CNI, which represent frequencies of centrosome number alterations. In both high and low CNI tumors, cells with extra centrosomes can be identified but the frequency of cells with one or zero centrosomes is higher in low CNI tumors. High CNI tumors (top purple cells) show decreased mesothelial clearance capacity and can show increased chemosensitivity. On the other hand, low CNI tumors, show increased mesothelial clearance capacity and low chemosensitivity, which accelerates tumor growth and peritoneal dissemination. Together, these conditions might facilitate tumor progression and relapse.

ACKNOWLEDGMENTS:

We are grateful to the patients that consent participating in this research and to the medical teams involved in their care. We thank S. Godinho, F. Gergely, S. McClelland, S. Taylor for sharing unpublished results, discussions and/or comments on the manuscript. We thank F. Edwards, V. Marthiens, S. Gemble, A. Goupil, D. Vargas and A. Simon for discussions and comments on the manuscript. We thank the Tissue Imaging (PICT-IBiSA) and Nikon Imaging Centre at Institut Curie, member of the French National Research Infrastructure France-BioImaging (ANR10-INBS-04). We thank A. Vieillefon, A. Rapinat and D. Gentien from the Genomics Platform of the translational research department at Institut Curie for cell line authentification.

The project was supported by a PIC project grant from the Labex CelTisphybio (2013, Institut Curie) and INCA PL-BIO grants (2015-PLBIO15-237) and the CNRS. The Basto lab is a member of the CelTisphybio labex.

AUTHOR CONTRIBUTION:

The project was initially designed and conceptualized by O.G., X. S. and R.B. with significant input from S.R.R. J.P.M. performed most experiments, including immunostaining, CNI quantifications of all the tissues and cell lines and the clearance assays; C.C was involved in setting the protocols for centrosome analysis in cells and tissues; A.H. help establishing the stable cell lines and performed *in vitro* chemotherapy experiments; B.M. and A.L. performed predictiveness curves and

provided expertise in statistical analysis. P.G. analysed gene expression levels and provided advice in statistical analysis. T.P. and M.H.S. help and advice on the HRD and ploidy status analysis. F.N. and D.D. performed all *in vivo* experiments. G.B. and V.B. did the pathological review of all the specimens; G.B. analyzed mitotic index; D.M and A.N. analysed ki67 in tumors; J.B. contributed to mesothelial clearance assays; O.G. performed activation assays. O.M. managed samples availability; X.S.-G. and A.V.S. provided human samples from pathology department of Institut Curie; C.B. and R.R. supplied surgical pieces to enlarge the cohort; R.R. provided expertise in ovarian cancers. F.M-G provided the OVCAR8 cell line, stress/fibrosis signature and advice in the methodology, as well as S.R.R. The work was supervised by O.G and R.B.

DECLARATION OF INTEREST:

M.H.S. and T.P. are inventors of the BRCAness/HRD (LST) genomic signature and Current exploitation of the patent is ongoing by Myriad Genetics. The other authors declare no competing interests.

REFERENCES:

1 Bettencourt-Dias, M. & Glover, D. M. Centrosome biogenesis and function: centrosomics brings new understanding. *Nature reviews. Molecular cell biology* **8**, 451-463, doi:10.1038/nrm2180 (2007).

2 Bornens, M. The centrosome in cells and organisms. *Science* **335**, 422-426, doi:10.1126/science.1209037 (2012).

3 Kushner, E. J. *et al.* Excess centrosomes disrupt endothelial cell migration via centrosome scattering. *J Cell Biol* **206**, 257-272, doi:10.1083/jcb.201311013 (2014).

4 Ogden, A., Rida, P. C. & Aneja, R. Heading off with the herd: how cancer cells might maneuver supernumerary centrosomes for directional migration. *Cancer Metastasis Rev* **32**, 269-287, doi:10.1007/s10555-012-9413-5 (2013).

5 Bornens, M. Centrosome composition and microtubule anchoring mechanisms. *Curr Opin Cell Biol* **14**, 25-34 (2002).

6 Gonczy, P. Centrosomes and cancer: revisiting a long-standing relationship. *Nat Rev Cancer* **15**, 639-652, doi:10.1038/nrc3995 (2015).

7 Boveri, T. Concerning the origin of malignant tumours by Theodor Boveri. Translated and annotated by Henry Harris. *J Cell Sci* **121 Suppl 1**, 1-84, doi:10.1242/jcs.025742 (2008).

8 Basto, R. *et al.* Centrosome amplification can initiate tumorigenesis in flies. *Cell* **133**, 1032-1042, doi:10.1016/j.cell.2008.05.039 (2008).

9 Sabino, D. *et al.* Moesin is a major regulator of centrosome behavior in epithelial cells with extra centrosomes. *Curr Biol* **25**, 879-889, doi:10.1016/j.cub.2015.01.066 (2015).

10 Coelho, P. A. *et al.* Over-expression of Plk4 induces centrosome amplification, loss of primary cilia and associated tissue hyperplasia in the mouse. *Open Biol* **5**, 150209, doi:10.1098/rsob.150209 (2015).

11 Sercin, O. *et al.* Transient PLK4 overexpression accelerates tumorigenesis in p53-deficient epidermis. *Nature cell biology* **18**, 100-110, doi:10.1038/ncb3270 (2016).

12 Levine, M. S. *et al.* Centrosome Amplification Is Sufficient to Promote Spontaneous Tumorigenesis in Mammals. *Dev Cell* **40**, 313-322.e315, doi:10.1016/j.devcel.2016.12.022 (2017).

13 Godinho, S. A. *et al.* Oncogene-like induction of cellular invasion from centrosome amplification. *Nature* **510**, 167-171, doi:10.1038/nature13277 (2014).

14 Arnandis, T. *et al.* Oxidative Stress in Cells with Extra Centrosomes Drives Non-Cell-Autonomous Invasion. *Dev Cell* **47**, 409-424 e409, doi:10.1016/j.devcel.2018.10.026 (2018).

15 Schnerch, D. & Nigg, E. A. Structural centrosome aberrations favor proliferation by abrogating microtubule-dependent tissue integrity of breast epithelial mammospheres. *Oncogene* **35**, 2711-2722, doi:10.1038/onc.2015.332 (2016).

16 Casenghi, M. *et al.* Polo-like kinase 1 regulates Nlp, a centrosome protein involved in microtubule nucleation. *Dev Cell* **5**, 113-125 (2003).

17 Ganier, O. *et al.* Structural centrosome aberrations promote non-cell-autonomous invasiveness. *Embo j* **37**, doi:10.15252/embj.201798576 (2018).

18 Berns, E. M. & Bowtell, D. D. The changing view of high-grade serous ovarian cancer. *Cancer Res* **72**, 2701-2704, doi:10.1158/0008-5472.can-11-3911 (2012).

19 Konstantinopoulos, P. A. & Awtrey, C. S. Management of ovarian cancer: a 75-year-old woman who has completed treatment. *JAMA* **307**, 1420-1429, doi:10.1001/jama.2012.269 (2012).

20 Pujade-Lauraine, E. *et al.* Bevacizumab combined with chemotherapy for platinum-resistant recurrent ovarian cancer: The AURELIA open-label randomized phase III trial. *J Clin Oncol* **32**, 1302-1308, doi:10.1200/jco.2013.51.4489 (2014).

21 Konstantinopoulos, P. A., Ceccaldi, R., Shapiro, G. I. & D'Andrea, A. D. Homologous Recombination Deficiency: Exploiting the Fundamental Vulnerability of Ovarian Cancer. *Cancer Discov* **5**, 1137-1154, doi:10.1158/2159-8290.cd-15-0714 (2015).

22 Vaughan, S. *et al.* Rethinking ovarian cancer: recommendations for improving outcomes. *Nat Rev Cancer* **11**, 719-725, doi:10.1038/nrc3144 (2011).

23 Torre, L. A. *et al.* Ovarian cancer statistics, 2018. *CA Cancer J Clin* **68**, 284-296, doi:10.3322/caac.21456 (2018).

24 Ramalingam, P. Morphologic, Immunophenotypic, and Molecular Features of Epithelial Ovarian Cancer. *Oncology (Williston Park)* **30**, 166-176 (2016).

25 Mateescu, B. *et al.* miR-141 and miR-200a act on ovarian tumorigenesis by controlling oxidative stress response. *Nat Med* **17**, 1627-1635, doi:10.1038/nm.2512 (2011).

26 TCGA. Integrated genomic analyses of ovarian carcinoma. *Nature* **474**, 609-615, doi:10.1038/nature10166 (2011).

27 Tothill, R. W. *et al.* Novel molecular subtypes of serous and endometrioid ovarian cancer linked to clinical outcome. *Clin Cancer Res* **14**, 5198-5208, doi:10.1158/1078-0432.ccr-08-0196 (2008).

28 Gentric, G. *et al.* PML-Regulated Mitochondrial Metabolism Enhances Chemosensitivity in Human Ovarian Cancers. *Cell Metab* **29**, 156-173 e110, doi:10.1016/j.cmet.2018.09.002 (2019).

29 Zhang, H. *et al.* Integrated Proteogenomic Characterization of Human High-Grade Serous Ovarian Cancer. *Cell* **166**, 755-765, doi:10.1016/j.cell.2016.05.069 (2016).

30 Lloyd, K. L., Cree, I. A. & Savage, R. S. Prediction of resistance to chemotherapy in ovarian cancer: a systematic review. *BMC Cancer* **15**, 117, doi:10.1186/s12885-015-1101-8 (2015).

31 Konstantinopoulos, P. A. & Matulonis, U. A. PARP Inhibitors in Ovarian Cancer: A Trailblazing and Transformative Journey. *Clin Cancer Res* **24**, 4062-4065, doi:10.1158/1078-0432.CCR-18-1314 (2018).

32 Goundiam, O. *et al.* Histo-genomic stratification reveals the frequent amplification/overexpression of CCNE1 and BRD4 genes in non-BRCAness high grade ovarian carcinoma. *Int J Cancer* **137**, 1890-1900, doi:10.1002/ijc.29568 (2015).

33 Conduit, P. T., Wainman, A. & Raff, J. W. Centrosome function and assembly in animal cells. *Nature reviews. Molecular cell biology* **16**, 611-624, doi:10.1038/nrm4062 (2015).

34 Godinho, S. A., Kwon, M. & Pellman, D. Centrosomes and cancer: how cancer cells divide with too many centrosomes. *Cancer Metastasis Rev* **28**, 85-98, doi:10.1007/s10555-008-9163-6 (2009).

35 Marthiens, V., Piel, M. & Basto, R. Never tear us apart--the importance of centrosome clustering. *J Cell Sci* **125**, 3281-3292, doi:10.1242/jcs.094797 (2012).
36 Breiman, L., Friedman, J., Olshen, R. & Stone, C. Classification and Regression Trees. *CRC Press* (1984).
37 Ganem, N. J., Godinho, S. A. & Pellman, D. A mechanism linking extra centrosomes to chromosomal instability. *Nature* **460**, 278-282, doi:10.1038/nature08136 (2009).
38 Pihan, G. A. Centrosome dysfunction contributes to chromosome instability, chromoanagenesis, and genome reprograming in cancer. *Front Oncol* **3**, 277, doi:10.3389/fonc.2013.00277 (2013).
39 Popova, T. *et al.* Genome Alteration Print (GAP): a tool to visualize and mine complex cancer genomic profiles obtained by SNP arrays. *Genome Biol* **10**, R128, doi:10.1186/gb-2009-10-11-r128 (2009).
40 Bielski, C. M. *et al.* Genome doubling shapes the evolution and prognosis of advanced cancers. *Nat Genet* **50**, 1189-1195, doi:10.1038/s41588-018-0165-1 (2018).
41 Zack, T. I. *et al.* Pan-cancer patterns of somatic copy number alteration. *Nat Genet* **45**, 1134-1140, doi:10.1038/ng.2760 (2013).
42 Lv, L. *et al.* Tetraploid cells from cytokinesis failure induce aneuploidy and spontaneous transformation of mouse ovarian surface epithelial cells. *Cell Cycle* **11**, 2864-2875, doi:10.4161/cc.21196 (2012).
43 Prat, J. Staging Classification for Cancer of the Ovary, Fallopian Tube, and Peritoneum: Abridged Republication of Guidelines From the International Federation of Gynecology and Obstetrics (FIGO). *Obstet Gynecol* **126**, 171-174, doi:10.1097/aog.0000000000000917 (2015).
44 Banerjee, S., Bookman, M. A. & Gore, M. in *Emerging Therapeutic Targets in Ovarian Cancer* (eds Stan Kaye, Robert Brown, Hani Gabra, & Martin Gore) 1-33 (Springer New York, 2011).
45 Huang, Y., Sullivan Pepe, M. & Feng, Z. Evaluating the predictiveness of a continuous marker. *Biometrics* **63**, 1181-1188, doi:10.1111/j.1541-0420.2007.00814.x (2007).
46 Chen, S. & Parmigiani, G. Meta-analysis of BRCA1 and BRCA2 penetrance. *J Clin Oncol* **25**, 1329-1333, doi:10.1200/jco.2006.09.1066 (2007).
47 Popova, T. *et al.* Ploidy and large-scale genomic instability consistently identify basal-like breast carcinomas with BRCA1/2 inactivation. *Cancer Res* **72**, 5454-5462, doi:10.1158/0008-5472.can-12-1470 (2012).
48 Manie, E. *et al.* Genomic hallmarks of homologous recombination deficiency in invasive breast carcinomas. *Int J Cancer* **138**, 891-900, doi:10.1002/ijc.29829 (2016).
49 Holland, A. J. *et al.* The autoregulated instability of Polo-like kinase 4 limits centrosome duplication to once per cell cycle. *Genes & development* **26**, 2684-2689, doi:10.1101/gad.207027.112 (2012).
50 Wong, Y. L. *et al.* Cell biology. Reversible centriole depletion with an inhibitor of Polo-like kinase 4. *Science* **348**, 1155-1160, doi:10.1126/science.aaa5111 (2015).
51 database, C. https://portals.broadinstitute.org/ccle.

52 Holland, A. J. *et al.* Polo-like kinase 4 controls centriole duplication but does not directly regulate cytokinesis. *Mol Biol Cell* **23**, 1838-1845, doi:10.1091/mbc.E11-12-1043 (2012).
53 Lambrus, B. G. *et al.* p53 protects against genome instability following centriole duplication failure. *J Cell Biol* **210**, 63-77, doi:10.1083/jcb.201502089 (2015).
54 Vitre, B. *et al.* Chronic centrosome amplification without tumorigenesis. *Proc Natl Acad Sci U S A* **112**, E6321-6330, doi:10.1073/pnas.1519388112 (2015).
55 Barbolina, M. V. Molecular Mechanisms Regulating Organ-Specific Metastases in Epithelial Ovarian Carcinoma. *Cancers (Basel)* **10**, doi:10.3390/cancers10110444 (2018).
56 Kipps, E., Tan, D. S. & Kaye, S. B. Meeting the challenge of ascites in ovarian cancer: new avenues for therapy and research. *Nat Rev Cancer* **13**, 273-282, doi:10.1038/nrc3432 (2013).
57 Cheng, H. W. *et al.* Centrosome guides spatial activation of Rac to control cell polarization and directed cell migration. *Life Sci Alliance* **2**, doi:10.26508/lsa.201800135 (2019).
58 Iwanicki, M. P. *et al.* Ovarian cancer spheroids use myosin-generated force to clear the mesothelium. *Cancer Discov* **1**, 144-157, doi:10.1158/2159-8274.cd-11-0010 (2011).
59 Marteil, G. *et al.* Over-elongation of centrioles in cancer promotes centriole amplification and chromosome missegregation. *Nature communications* **9**, 1258, doi:10.1038/s41467-018-03641-x (2018).
60 Marthiens, V. *et al.* Centrosome amplification causes microcephaly. *Nature cell biology* **15**, 731-740, doi:10.1038/ncb2746 (2013).
61 Zyss, D. & Gergely, F. Centrosome function in cancer: guilty or innocent? *Trends in cell biology* **19**, 334-346, doi:10.1016/j.tcb.2009.04.001 (2009).
62 Kwon, M. *et al.* Mechanisms to suppress multipolar divisions in cancer cells with extra centrosomes. *Genes & development* **22**, 2189-2203, doi:10.1101/gad.1700908 (2008).
63 Weidle, U. H., Birzele, F., Kollmorgen, G. & Rueger, R. Mechanisms and Targets Involved in Dissemination of Ovarian Cancer. *Cancer genomics & proteomics* **13**, 407-423 (2016).
64 Worzfeld, T. *et al.* The Unique Molecular and Cellular Microenvironment of Ovarian Cancer. *Front Oncol* **7**, 24, doi:10.3389/fonc.2017.00024 (2017).
65 Niedbala, M. J., Crickard, K. & Bernacki, R. J. Interactions of human ovarian tumor cells with human mesothelial cells grown on extracellular matrix. An in vitro model system for studying tumor cell adhesion and invasion. *Exp Cell Res* **160**, 499-513 (1985).
66 Mason, J. M. *et al.* Functional characterization of CFI-400945, a Polo-like kinase 4 inhibitor, as a potential anticancer agent. *Cancer Cell* **26**, 163-176, doi:10.1016/j.ccr.2014.05.006 (2014).
67 Pillay, N. *et al.* DNA Replication Vulnerabilities Render Ovarian Cancer Cells Sensitive to Poly(ADP-Ribose) Glycohydrolase Inhibitors. *Cancer Cell* **35**, 519-533 e518, doi:10.1016/j.ccell.2019.02.004 (2019).
68 Lisio, M. A., Fu, L., Goyeneche, A., Gao, Z. H. & Telleria, C. High-Grade Serous Ovarian Cancer: Basic Sciences, Clinical and Therapeutic Standpoints. *Int J Mol Sci* **20**, doi:10.3390/ijms20040952 (2019).

69 Gao, H. *et al.* High-throughput screening using patient-derived tumor xenografts to predict clinical trial drug response. *Nat Med* **21**, 1318-1325, doi:10.1038/nm.3954 (2015).

Figure 1 - Morteton et al.

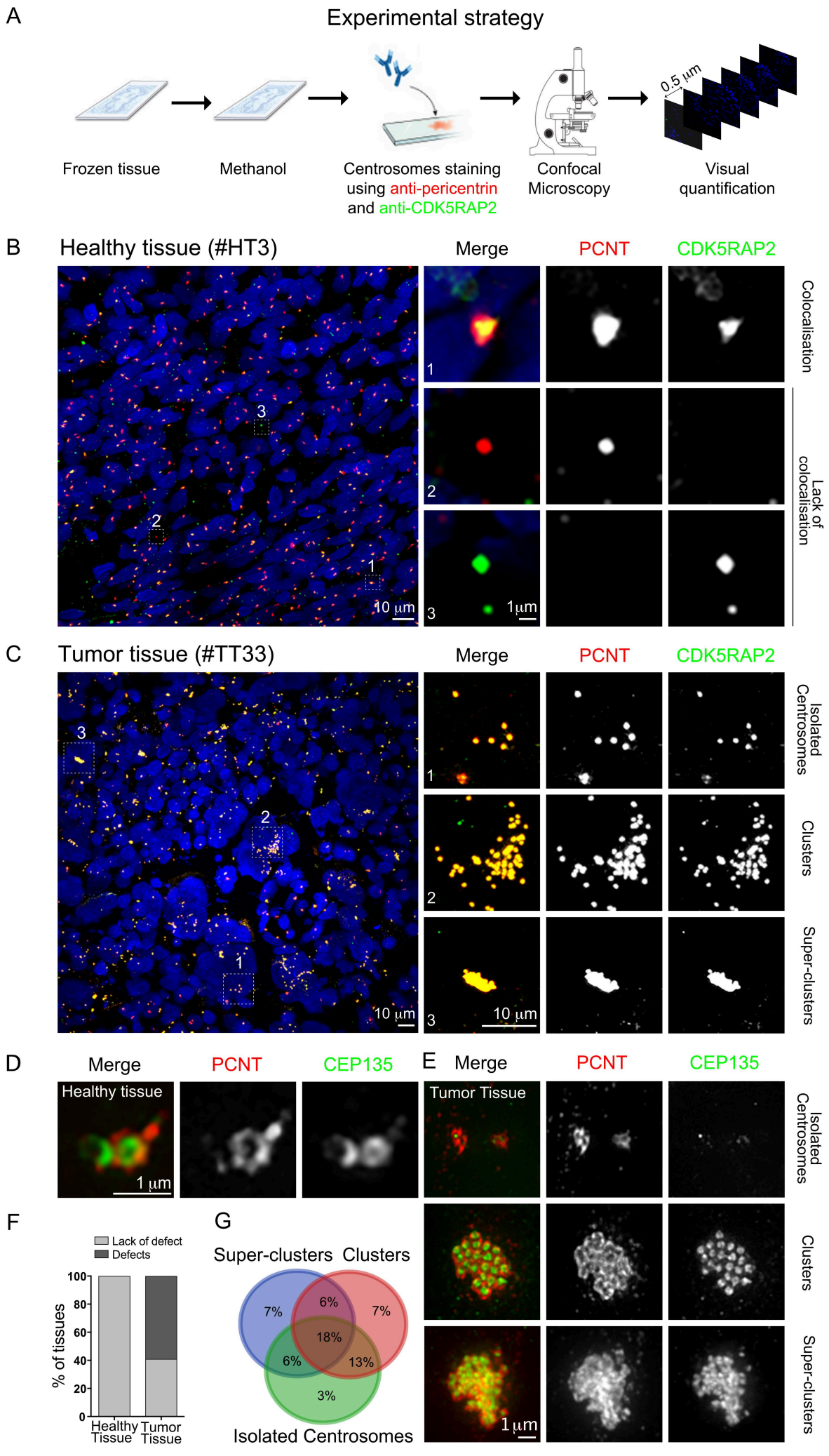

Figure2 - Morelon et al.

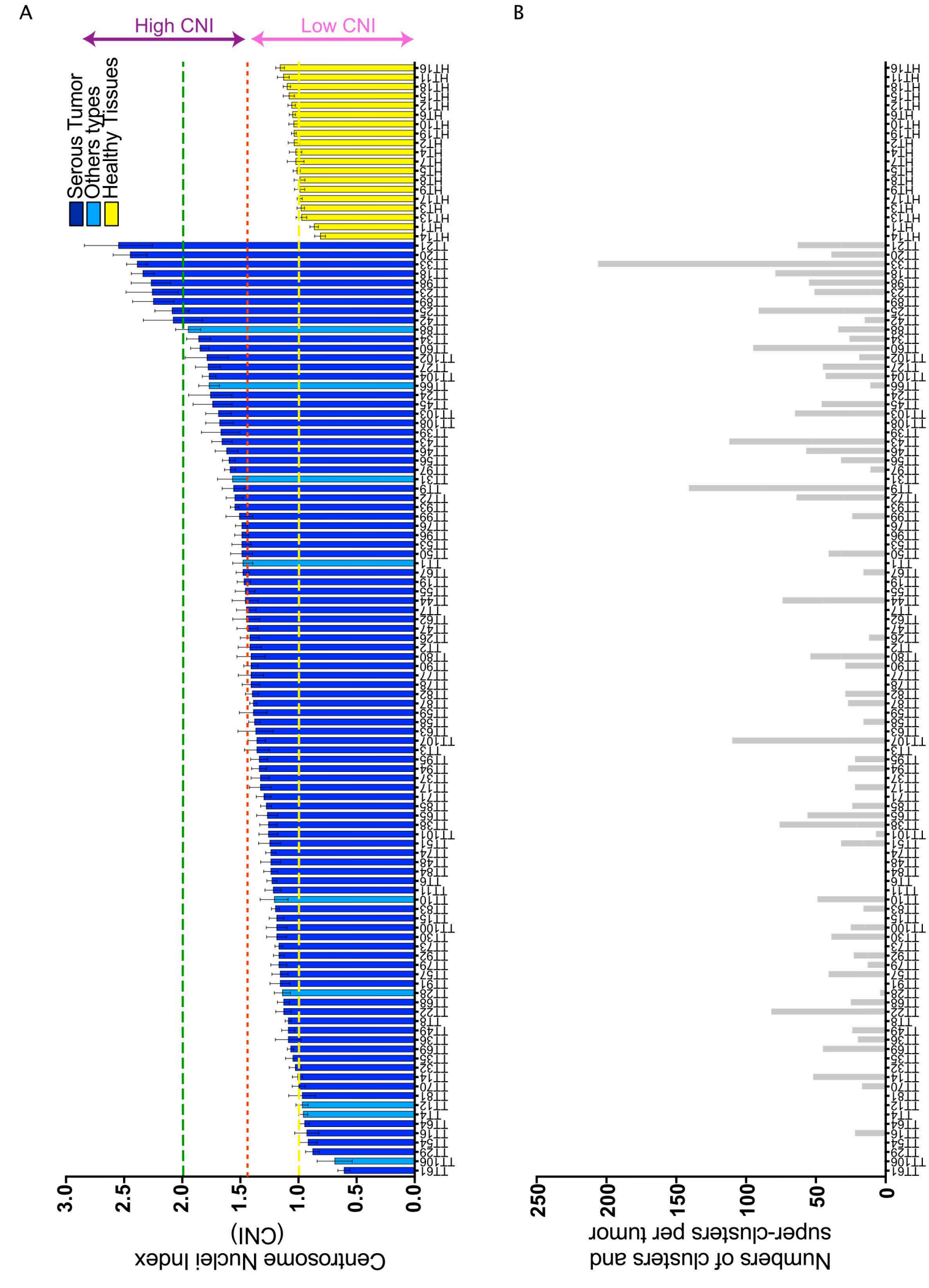

Figure 3 - Morelon et al.

A

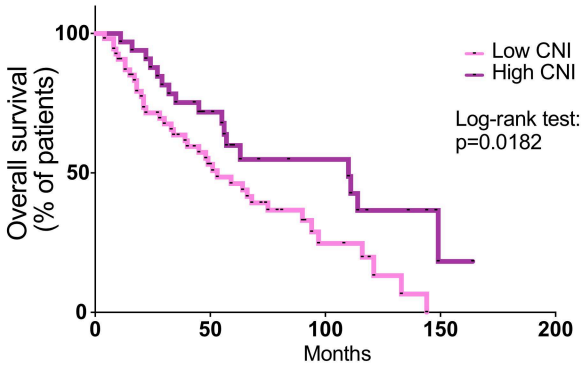

B

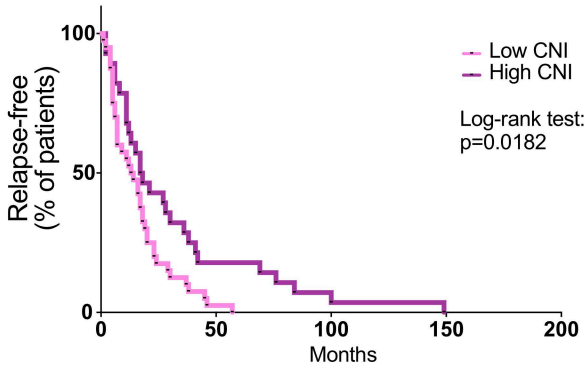

C

	CNI status		
	Low (40 tumors)	High (27 tumors)	p[1]
HRP	22 (55%)	7 (26%)	0.0245
HRD	18 (45%)	20 (74%)	

D

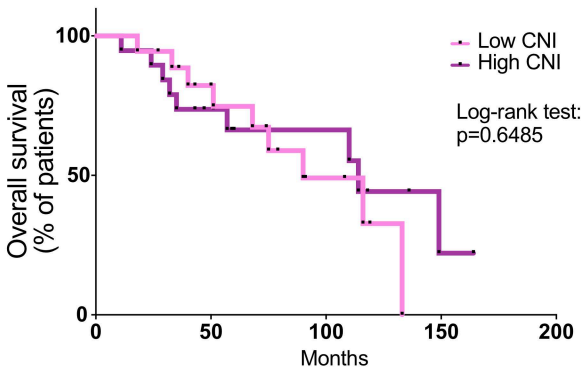

E

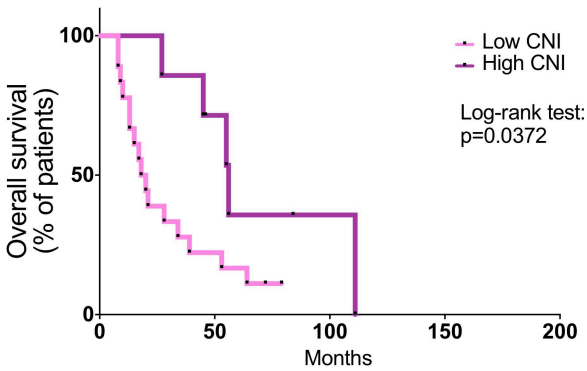

Figure 4 - Morretton et al.

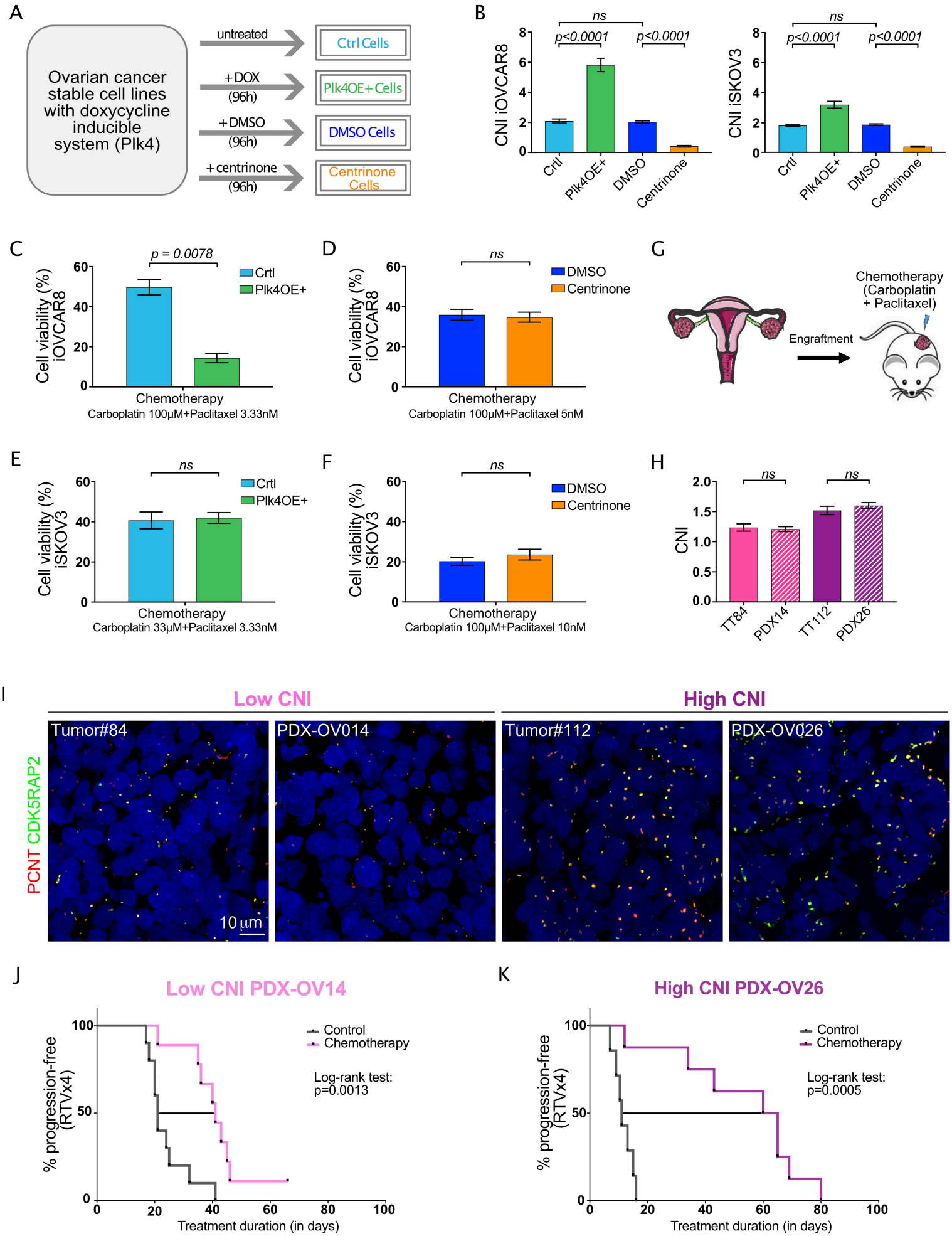

Figure 5 - Morfoton et al.

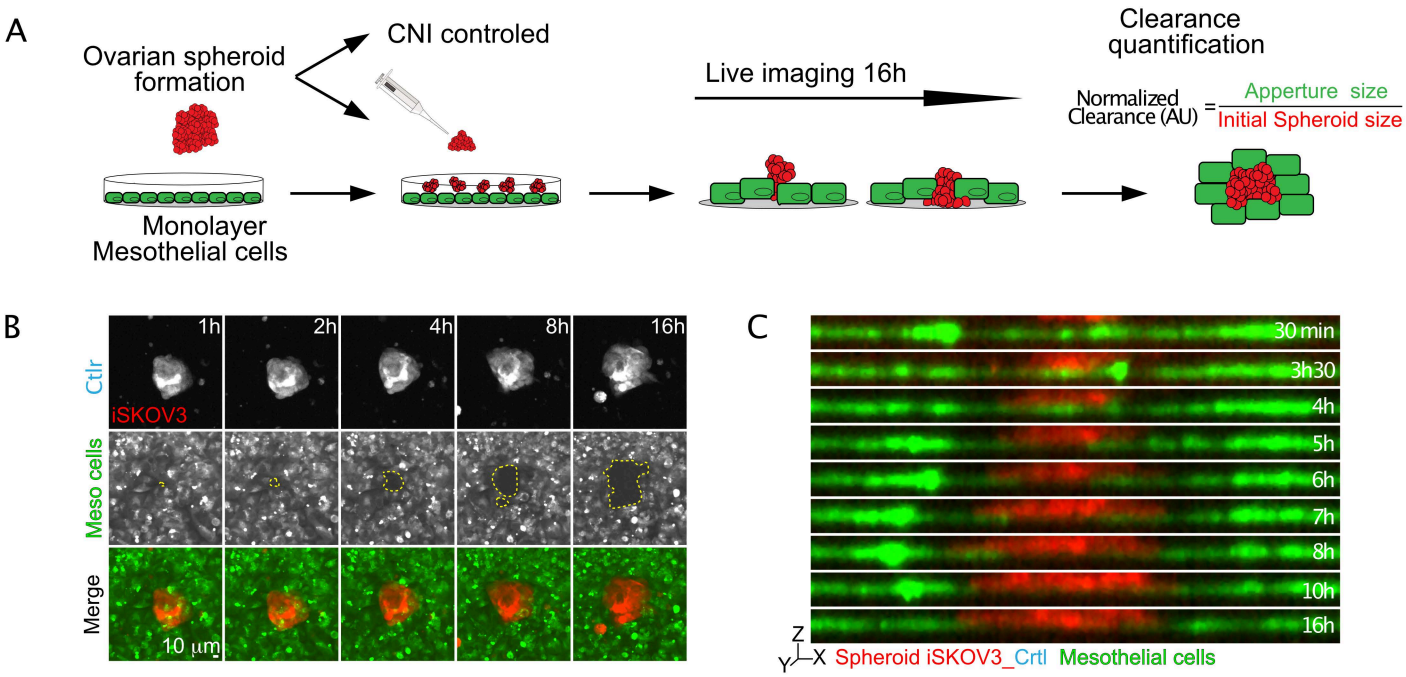

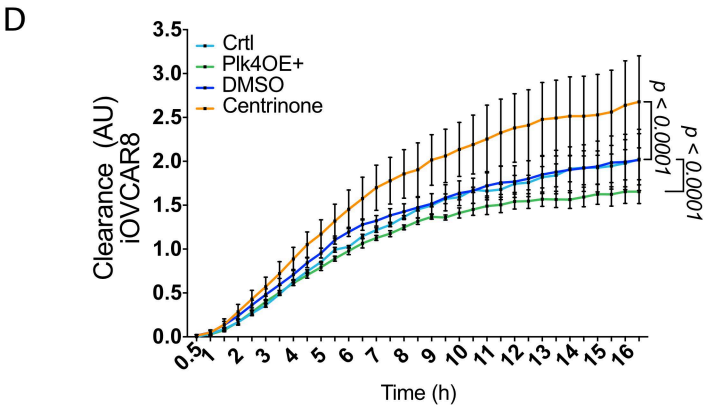

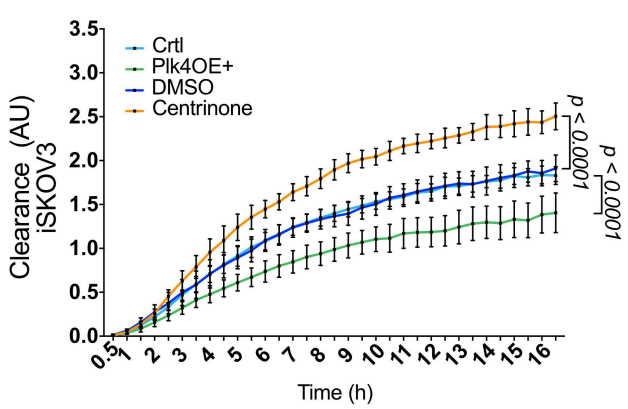

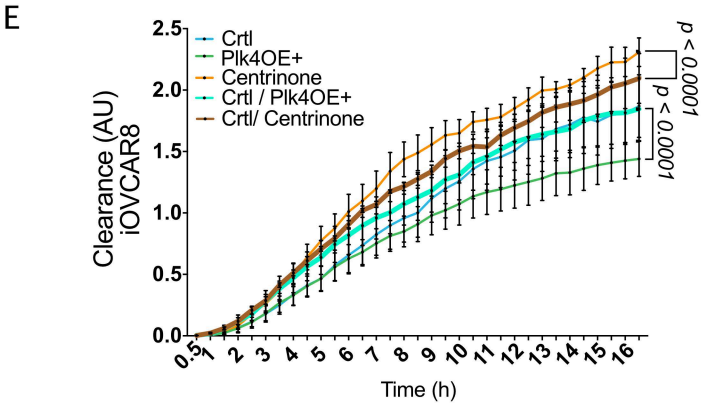

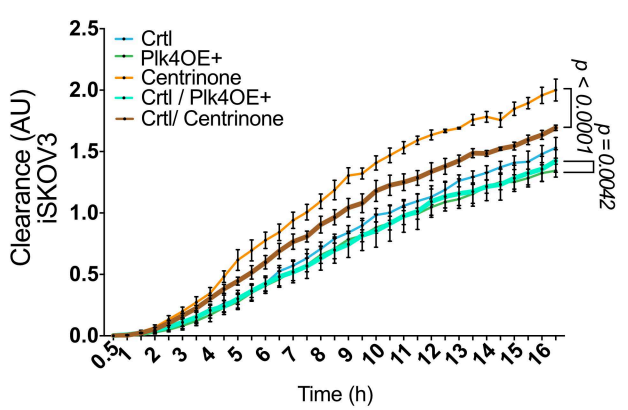

Figure 6 - Morretton et al.